Recombination in Quantum Dot Sensitized Solar Cells

IVÁN MORA-SERÓ,*,† SIXTO GIMÉNEZ,†
FRANCISCO FABREGAT-SANTIAGO,† ROBERTO GÓMEZ,‡
QING SHEN,§ TARO TOYODA,*,§ AND JUAN BISQUERT*,†

†Grup de Dispositius Fotovoltaics i Optoelectrònics, Departament de Fisica, Universitat Jaume I, 12071 Castelló, Spain, ‡Departament de Química-Física i Institut Universitari d'Electroquímica, Universitat d'Alacant, Ap. 99, E-03080 Alacant, Spain, §Department of Applied Physics and Chemistry, The University of Electro-Communications, 1-5-1 Chofugaoka, Chofu, Tokyo 182-8585, Japan

CONSPECTUS

Quantum dot sensitized solar cells (QDSCs) have attracted significant attention as promising third-generation photovoltaic devices. In the form of quantum dots (QDs), the semiconductor sensitizers have very useful and often tunable properties; moreover, their theoretical thermodynamic efficiency might be as high as 44%, better than the original 31% calculated ceiling. Unfortunately, the practical performance of these devices still lags behind that of dye-sensitized solar cells. In this Account, we summarize the strategies for depositing CdSe quantum dots on nanostructured mesoporous TiO_2 electrodes and discuss the methods that facilitate improvement in the performance and stability of QDSCs.

One particularly significant factor for solar cells that use polysulfide electrolyte as the redox couple, which provides the best performance among QDSCs, is the passivation of the photoanode surface with a ZnS coating, which leads to a dramatic increase of photocurrents and efficiencies. However, these solar cells usually show a poor current−potential characteristic, so a general investigation of the recombination mechanisms is required for improvements. A physical model based on recombination through a monoenergetic TiO_2 surface state that takes into account the effect of the surface coverage has been developed to better understand the recombination mechanisms of QDSCs. The three main methods of QD adsorption on TiO_2 are (i) in situ growth of QDs by chemical bath deposition (CBD), (ii) deposition of presynthesized colloidal QDs by direct adsorption (DA), and (iii) deposition of presynthesized colloidal QDs by linker-assisted adsorption (LA).

A systematic investigation by impedance spectroscopy of QDSCs prepared by these methods showed a decrease in the charge-transfer resistance and increased electron lifetimes for CBD samples; the same result was found after ZnS coating because of the covering of the TiO_2 surface. The increase of the lifetime with the ZnS treatment has also been checked independently by open-circuit potential (V_{oc}) decay measurements. Despite the lower recombination rates by electron transfer to electrolyte as well as the higher light absorption of CBD samples, only a moderate increase of photocurrent compared with colloidal QD samples is obtained, indicating the presence of an additional, internal recombination pathway in the closely packed QD layer.
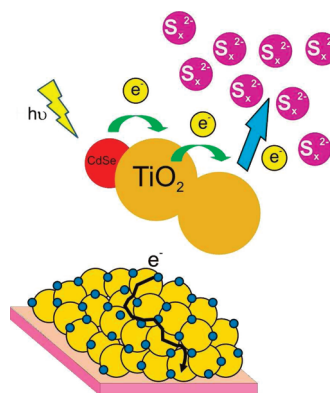
1. Introduction

Quantum dot sensitized solar cells (QDSCs) constitute one of the most promising approaches to third generation solar cells.[1−4] The intrinsic attractive properties of QDs (tunable band gap,[5] high extinction coefficients,[5,6] and large intrinsic dipole moment[7,8]) offer certain advantages over metall-organic dyes as alternative light absorbers. Moreover, the demonstration of multiple exciton generation by impact ionization in colloidal QDs[9,10] could push the thermodynamic efficiency limit of these devices up to 44%[2] instead of the
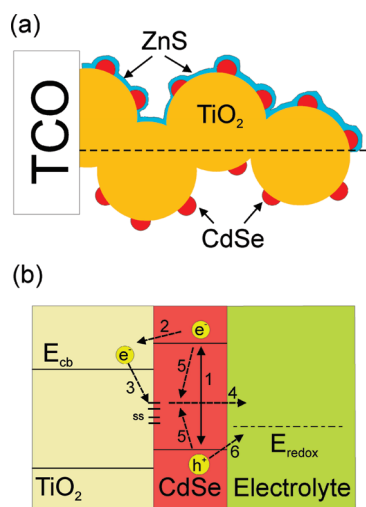
(a)

(b)

FIGURE 1. (a) Scheme of a TiO$_2$ nanostructured film deposited on transparent conducting oxide, sensitized with CdSe QDs (bottom) and covered with a ZnS layer (top) and (b) energetic diagram of CdSe-sensitized TiO$_2$ in contact with electrolyte, showing the main electronic processes at the interface in a QDSC: (1) photoexcitation, (2) electron injection, (3) trapping of a free electron at a surface state, (4) charge transfer of a trapped electron toward electrolyte acceptor, (5) recombination in the absorber semiconductor, and (6) hole extraction.

current 31% of the Schockley−Queisser detailed balance limit. Although the efficiencies of QDSCs lag behind those of dye-sensitized solar cells (DSCs)[11] (DSC currently exceeds 11% at 1 sun illumination[12]), QD-sensitized nanostructured solar cells are attracting increasing attention among researchers and are progressing very rapidly.[13−15]

Several aspects of the sensitization of nanostructured solar cells with inorganic semiconductors and QDs have been recently reviewed.[3,4] Hodes[4] concluded that the surface states need to be passivated and the recombination in the absorber layer reduced. In this Account, we aim to progress in this direction by proposing a scheme of the operational mechanisms taking place in working devices. QDSC performance has been usually hampered by very poor current−potential ($j−V$) characteristics, as represented by low fill factors (FF). We summarize the methods usually employed to apply QD sensitization and ZnS coating layers. Strategies for conformal coating of the metal oxide with nanometric barriers have been widely used in DSC with molecular sensitizers.[16−18] Coating of QDSCs, as indicated in the upper part of Figure 1a, can partially overcome the recombination losses leading to higher photocurrents. In fact, the ZnS coating has been demonstrated to almost double the obtained photocurrents,[14,19,20] although the exact passivation mechanism is not well understood. In this Account, we describe a physical model, based on the concept of band unpinning,[21] that allows recognition of the pres-

ence of surface states and the effects of blocking layers from the analysis of capacitance−voltage curves of the solar cell. A systematic analysis of the recombination process in QDSCs, Figure 1b, with QDs adsorbed by different methods facilitates the interpretation of the features of $j−V$ curves. A recombination pathway through monoenergetic surface states in TiO$_2$ is shown to play a major role in the low FF obtained for QDSCs with polysulfide aqueous electrolyte.

2. Strategies for Sensitization of Nanostructured Solar Cells with Quantum Dots

Several configurations have been suggested for the application of semiconductor QDs in solar cells, including those based on 3D QD arrays or on blends of QDs and conducting polymers.[1,22] Another configuration, which is discussed in this Account, is directly based on the DSC but using QDs attached to the semiconductor oxide matrix as light absorbers. The sensitization of large band gap semiconductors (oxides) with lower band gap semiconductors dates back to 1984.[23] Systematic studies along these lines appeared in the 1990s together with the first QDSCs. Initially, chalcogenide QDs, directly grown into the nanoporous layer by either chemical or electrochemical methods, were used as sensitizers.[7,24] The first reported solar cell using presynthesized QDs was based on InP QDs attached to TiO$_2$.[25]

Accordingly, the sensitization of a wide gap nanostructured semiconductor electrode (TiO$_2$, ZnO) with QDs can be performed mainly through two different approaches: (1) direct growth of the semiconductor QDs on the electrode surface by chemical reaction of ionic species using the methods of chemical bath deposition (CBD)[13,14,19,26] or successive ionic layer adsorption and reaction (SILAR)[27,28] and (2) using presynthesized colloidal QDs attached to the electrode material by a bifunctional linker molecule.[29−34] Additionally, some studies using a combination of both linked colloidal QDs and CBD have been carried out.[35,36] The first approach involves a nucleation and growth mechanism leading to a high coverage of the effective TiO$_2$ surface but rendering rather difficult the control of the size distribution of the deposited QDs. On the other side, the attachment of colloidal QDs through molecular wires leads to precise morphological characteristics (shape and size) of the semiconductor nanocrystals subsequently leading to potentially enhanced properties compared with CBD.

An alternative method (3) to attach the colloidal QDs onto the TiO$_2$ surface without the need for molecular linkers is

termed direct adsorption (DA). This procedure has already been employed to sensitize TiO_2 with CdSe,[37] InAs,[38] and InP,[25] although the obtained photocurrents at 1 sun intensity were low. A significant increase of the obtained photocurrents using this adsorption strategy has been recently reported.[20,34] However, at present, the use of presynthesized colloidal QDs leads to less efficient solar cell devices compared with directly grown QDs. One possible explanation is that directly adsorbed colloidal QDs provides a low surface coverage of about 14%.[39] It is obvious that a higher surface coverage of colloidal QDs on the TiO_2 substrate is a "must" to improve the efficiencies of QDSCs.

3. Progress in QDSC Configurations and Efficiency

The most efficient redox system developed for DSC is the I^-/I_3^- system. Unfortunately, cadmium chalcogenides, the most used QD materials within this context, are not chemically compatible with this redox electrolyte. Consequently, modifications in the cell configuration and different redox couples and electrolytes have been tested for QDSCs. In order to use the I^-/I_3^- redox electrolyte, the QDs must be protected, for example, with an amorphous TiO_2 coating. This approach has led to a 1.24% efficiency for CdS QDSCs.[40] Using Co^{2+}/Co^{3+} redox systems, Lee et al.[15] reported a 1.17% efficiency at 1 sun illumination. These two approximations lead to good fill factors (FF), ranging between 0.6 and 0.7, but with relatively low photocurrents.

The highest photocurrents for QDSCs have been obtained using a polysulfide redox system in aqueous electrolyte.[13,14,20] The stability of QDs in polysulfide electrolyte is discussed in Supporting Information. These QDSCs have generally suffered from very poor fill factors (conventionally 0.2−0.4). Chemical species coming from water constitute favorable recombination paths for electrons via surface states of TiO_2.[41] The partial substitution of water by methanol in the polysulfide redox electrolytes has been demonstrated to slightly increase the obtained photocurrents investigated although the FFs are still very low (around 0.40).[42]

In recent years, Toyoda's group has been focusing on the preparation and characterization of CdSe QDs that were deposited by using the CBD method and applied to sensitize nanostructured TiO_2 electrodes of various morphologies, including nanoparticles, nanotubes, and inverse opals. They have been studying their optical absorption, photoelectrochemical and photovoltaic properties, and ultrafast carrier dynamics.[43−49] The CdSe QDs were coated with ZnS, and the
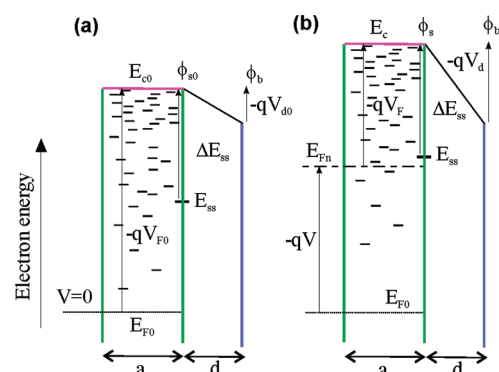

FIGURE 2. Scheme of a TiO_2 semiconductor layer with exponential DOS, a surface state, and a dielectric layer: (a) equilibrium; (b) negative bias potential applied in the substrate, which causes a rise of the Fermi level and a shift of the conduction band by charging the surface state.

effects of this coating on the photovoltaic properties were studied. There are few reports in which a ZnS coating has been applied to CdSe QD-sensitized TiO_2 solar cells. On the other hand, ZnS capped CdSe in core−shell QDs has been used for strong photoluminescence applications.[50]

The FF of polysulfide QDSCs can be further increased by selecting an adequate counter electrode material. In a recent study,[20] we showed that the use of Cu_2S or Au instead of the conventional Pt counter electrode, led to 0.48 and 0.42 FF, respectively, although these values are still low. See Supporting Information for further discussion on this topic.

4. Effect of Deep Monoenergetic Surface States

The characteristic pattern of the charge transfer resistance (i.e., resistance of the recombination process of the electrons from the TiO_2 electrode with the electrolyte) when a recombination pathway through a monoenergetic surface state exists has been previously investigated.[41] A minimum in the charge transfer resistance is obtained when the Fermi level crosses the surface state. Additional evidence for surface states can be obtained from the capacitance. We next analyze how the behavior of the chemical capacitance[51] in nanostructured semiconductors is influenced by the surface state charging and, importantly, the additional modification of the capacitance by a dielectric layer between the semiconductor and solution.[52]

With reference to Figure 2, we consider a semiconductor (TiO_2) layer of thickness a, deposited on a conducting substrate and covered with a dielectric layer of thickness d and dielectric constant ε, which is in contact with the electrolyte. In the bulk TiO_2, we assume an exponential distribution of

localized states (DOS) in the bandgap as described by the expression[53]

$$g(E) = \frac{N_L}{k_B T_0} \exp[(E - E_c)/(k_B T_0)] \qquad (1)$$

Here E_c is the energy of the conduction band edge, N_L is the total volume density, k_B is Boltzmann's constant, and T_0 is a parameter with temperature units that determines the depth of the distribution. In addition, we assume a surface state of energy $E_{ss} = E_c - \Delta E_t$ and concentration (per unit surface) N_{ss}. We denote the Fermi level of electrons, E_{F_n}, and E_{F_0} the equilibrium Fermi level; therefore the applied bias voltage is $-qV = E_{F_n} - E_{F_0}$. When the Fermi level raises in TiO$_2$, the surface state becomes increasingly charged. This changes the voltage drop across the dielectric layer, which is given by $V_d = \phi_s - \phi_b$, where ϕ_s is the electrostatic potential at the semiconductor/dielectric layer interface and ϕ_b is the potential in the bulk electrolyte. Therefore it is useful to express the bias potential in two components.[54] We first define V_F, the potential related to the displacement of the Fermi level with respect to the conduction band (i.e., the chemical potential):

$$qV_F = E_c - E_{F_n} \qquad (2)$$

Since $E_c = -q\phi_s$, it is easy to show that

$$V = V_F + V_d - (V_{F_0} + V_{d_0}) \qquad (3)$$

This means that the potential applied in the substrate is used both to displace the electronic Fermi level and to increase the potential drop across the dielectric layer, see Figure 2. Note that the total potential in the solar cell, V_{ap}, may contain additional contributions (electrolyte, counter electrode, etc.). Assuming that the Fermi level of trapped electrons is the same as the Fermi level of free electrons in the conduction band,[41] the negative charge in the surface state is

$$Q_{ss} = qN_{ss}f(E_{ss} - E_{F_n}) \qquad (4)$$

where f is the Fermi−Dirac distribution

$$f(E_{ss} - E_{F_n}) = \frac{1}{1 + \exp[(E_{ss} - E_{F_n})/(k_B T)]} \qquad (5)$$

The compensating ionic charge in the dielectric surface is given by $Q_i = C_d V_d$, where the capacitance has the form $C_d = \varepsilon\varepsilon_0/d$. Therefore we obtain

$$V_d = \frac{qd}{\varepsilon\varepsilon_0} \frac{N_{ss}}{1 + e^{-(\Delta E_t + qV_F)/(k_B T)}} \qquad (6)$$

Figure 3a shows the step of the voltage in the dielectric layer (i.e., the band unpinning due to electrons in the surface
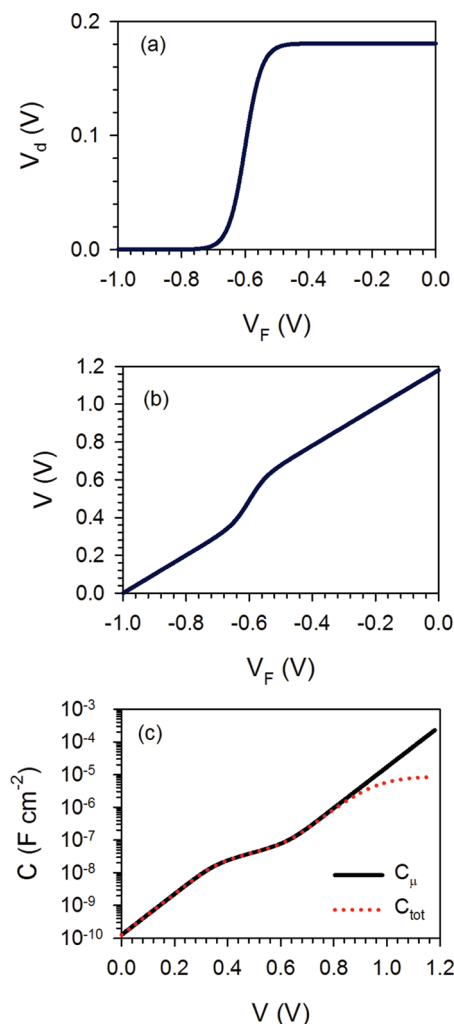

FIGURE 3. Representation of the variation of (a) potential drop in the dielectric, (b) applied potential, and (c) capacitance in the charging of a semiconductor layer with exponential DOS, a surface state, and a dielectric layer. V is the external bias potential. Parameters used in the simulation: $a = 10^{-6}$ cm; $d = 10^{-7}$ cm; $\varepsilon = 10$; $N_L = 10^{20}$ cm^{-3}; $N_{ss} = 10^{13}$ cm^{-2}; $\Delta E_t = 0.6$ eV; $T = 300$ K; $T_0 = 800$ K.

state) that occurs when the Fermi level crosses the energy level of the surface state. By eq 3, we obtain the dependence of the bias voltage $V(V_F)$, and this is shown in Figure 3b. From eq 1, we can obtain the chemical capacitance of the TiO$_2$ layer[51,53]

$$C_\mu = \frac{N_{sc}q^2}{k_B T_0} e^{qV_F/(k_B T_0)} \qquad (7)$$

and this is represented in Figure 3c. When $E_{F_n} \approx E_{ss}$, the step of the voltage in the dielectric layer brings up the conduction band. In this domain of bias voltage, the internal chemical potential V_F is stationary, and hence a plateau of the chemical capacitance occurs.
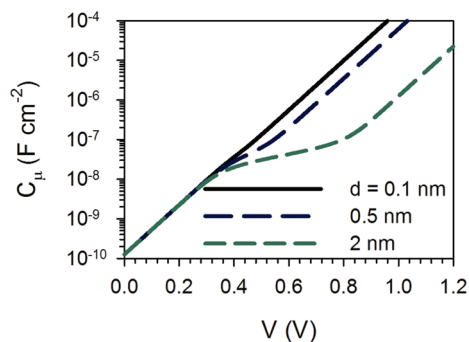
FIGURE 4. Representation of the variation of chemical capacitance with respect to the external bias potential in the charging of a semiconductor layer with exponential DOS, a surface state, and a dielectric layer. Parameters used in the simulation: $a = 10^{-6}$ cm; $\varepsilon = 10$; $N_L = 10^{20}$ cm^{-3}; $N_{ss} = 10^{13}$ cm^{-2}; $\Delta E_t = 0.6$ eV; $T = 300$ K; $T_0 = 800$ K; d varies as indicated.

TABLE 1. Photovoltaic Properties of QDSC under 1 Sun Illumination (AM 1.5 G)

cell	V_{oc} (V)	j_{sc} (mA/cm^2)	FF	efficiency (%)
DA−ZnS−Au	0.48	4.48	0.29	0.62
DA−ZnS−Pt	0.49	5.10	0.28	0.72
DA−Au	0.43	1.93	0.29	0.24
DA−Pt	0.46	3.12	0.28	0.40
CBD−ZnS−Au	0.49	4.70	0.37	0.85
CBD−ZnS−Pt	0.53	5.91	0.33	1.04
CBD−Au	0.39	1.09	0.49	0.21
LA−ZnS−Au	0.49	2.88	0.29	0.41
LA−ZnS−Pt	0.49	2.92	0.24	0.35
LA−Au	0.47	1.42	0.22	0.14
LA−Pt	0.42	2.35	0.27	0.26

The measured low-frequency capacitance in impedance spectra (IS) corresponds to the series combination

$$C = (C_\mu^{-1} + C_d^{-1})^{-1} \tag{8}$$

The total capacitance shows a saturation when the chemical capacitance becomes larger than C_d, Figure 3c. The voltage drop V_d is proportional to the thickness of the dielectric layer; therefore the plateau of the chemical capacitance becomes larger when the thickness of the dielectric d increases, as shown in Figure 4.

5. Steady-State Characteristics of QDCSs

The performance of a range of QDSCs in different configurations (deposition method − covering layer − counterelectrode) is indicated in Table 1. All details about the methods of preparation are given in Supporting Information. It is well-known that TiO$_2$ exhibits a nearly monoenergetic surface state ∼0.4 eV below its conduction band (CB)[55] in addition of the continuous exponential distribution of eq 1. This level can be easily recognized by cyclic voltammetry measurements (negative-going scan) as a peak in the exponentially growing cathodic current.[56] Such peak is also observed in QDSCs under dark
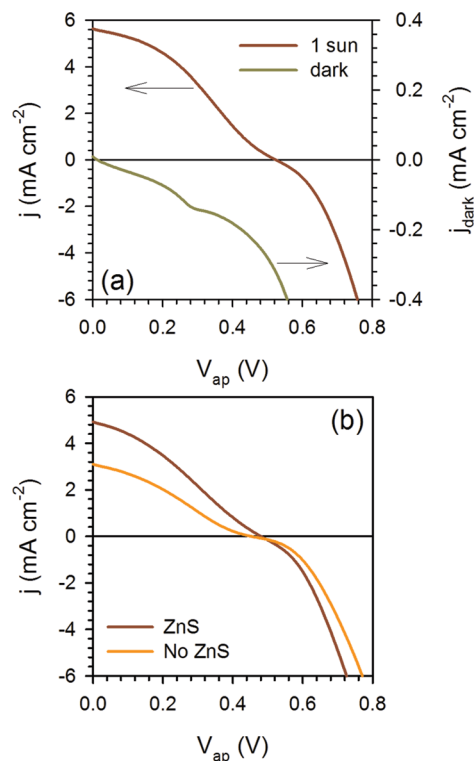

FIGURE 5. (a) Current density−potential (j−V) curve of a CBD QDSC coated with ZnS under 1 sun illumination and in the dark. Cell configuration: FTO + buffer + TiO$_2$ + CBD QDs + poly + Pt counter. (b) j−V curves of a DA QDSC under 1 sun illumination with and without ZnS coating. Cell configuration: FTO + buffer + TiO$_2$ + DA QDs + ZnS/no ZnS +polysulfide + Pt counter.

conditions, Figure 5a, and it is responsible for the S-shape observed for the devices under illumination, Figure 5b, which notably reduces the FF of the solar cell. This peak indicates the presence of an alternative recombination pathway of electrons photoinjected into TiO$_2$ with the electrolyte through a monoenergetic surface state, that is, process 4 of Figure 1b, together with the standard recombination pathway of electrons in the CB or shallow surface states of TiO$_2$.[57,58]

Figure 5b shows a typical j−V curve corresponding to a QDSC illustrating the effect of the ZnS coating for DA-deposited QDs. The covering causes a clear increase of both open-circuit voltage, V_{oc}, and short-circuit current, j_{sc}, leading to a significant increase of efficiency (Table 1). A similar trend was observed for QDs deposited by CBD and LA after ZnS coating, although the effect of the ZnS coating is considerably weaker for the LA cells (Table 1), where the efficiencies are also lower compared with those of DA and CBD cells. This is most probably because the amount of QDs deposited by LA on the nanostructured TiO$_2$ is significantly lower than that with DA and, especially, CBD.[39]
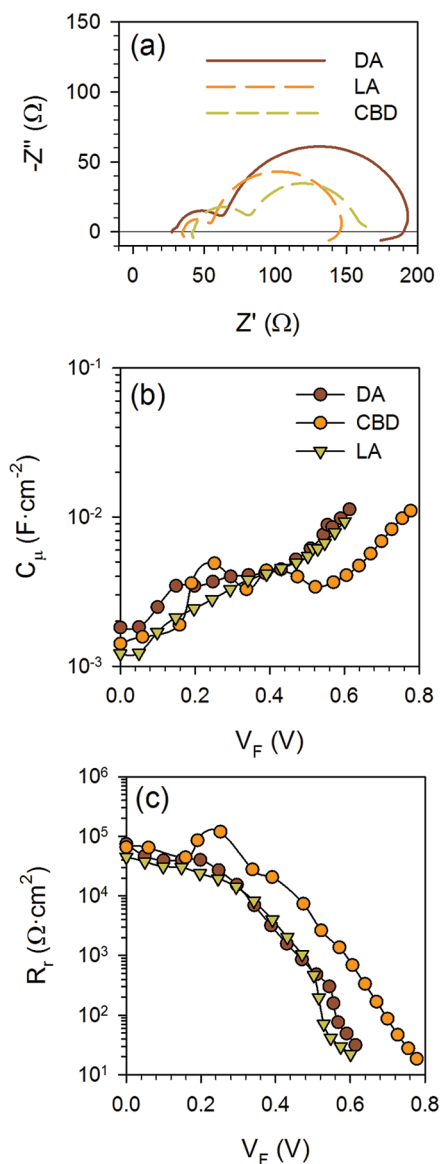
FIGURE 6. Experimental results of IS of QDSC with configuration FTO + buffer + TiO_2 + QDs + ZnS + polysulfide + Au counter, with QDs deposited by DA, LA, and CBD: (a) impedance spectra at 0.8 V in the dark; (b) chemical capacitance and (c) recombination resistance, as a function of the voltage associated with the second arc of panel a.

Reflectance measurements indicate a slight increase of light absorption after ZnS coating the QDSCs, see Supporting Information.

6. Dynamic Measurements of QDSCs

IS has been amply used in DSCs to determine electronic processes and recombination dynamics.[58,59] We discuss the results of IS measurements on the specimens listed in Table 1. Impedance spectra are characterized by the presence of two semiarcs, Figure 6a, that were treated using the equivalent circuit shown in Figure S3, Supporting Information. The high-
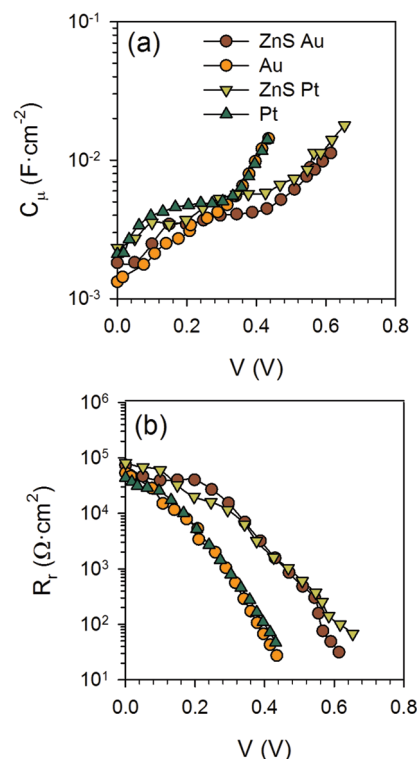

FIGURE 7. (a) Chemical capacitance and (b) recombination resistance as a function of voltage in a QDSC with directly adsorbed QDs (DA), with and without ZnS coating, using Au and Pt as the counter electrode materials. IS under dark conditions.

frequency semiarc is related to the counter electrode material and presents higher resistances than the I^-/I_3^- redox and the platinized counter electrodes conventionally used in DSC.[32] The low-frequency arc includes the chemical capacitance of nanostructured TiO_2 (C_μ), modified as indicated in eq 8, and charge transfer resistance between TiO_2 and the polysulfide electrolyte (R_r). The latter quantity provides important information on steady-state recombination flux. It has been systematically observed that colloidal QDSCs based on ZnS treated electrodes exhibit negative capacitance behavior at low frequencies,[60] in contrast to nontreated photoanodes. This indicates the existence of a nonconventional charge accumulation effect, where the increase of charge diminishes as the Fermi level increases, a process that is very probably caused by surface states.[61]

Figures 6−9 show the recombination resistance and chemical capacitance of TiO_2 versus potential V for several QDSCs. The potential drop in series resistance, in the counter electrode and in the electrolyte, has been subtracted from the total potential V_{ap}, which removes the effect of the counter electrode on both R_r and C_μ, see Figure 7a.

The general characteristic of the chemical capacitance is shown in Figure 6b for ZnS coated cells. We find the standard exponential rise of the chemical capacitance[53] at forward bias
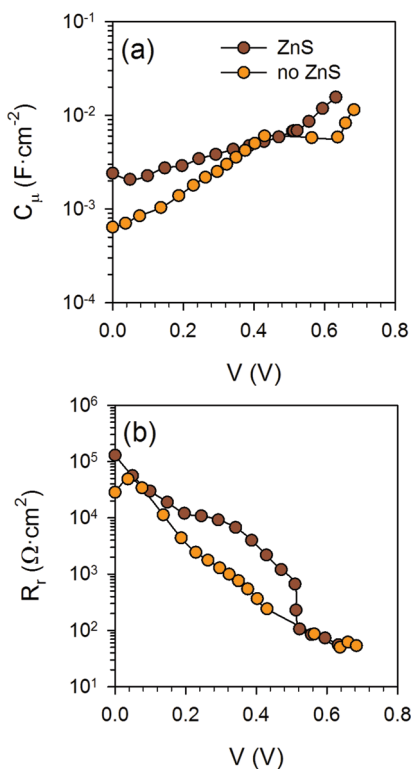
FIGURE 8. (a) Chemical capacitance and (b) recombination resistance as a function of voltage in a QDSC with linker-assisted adsorbed QDs (LA), with and without ZnS coating, using Pt as the counter electrode material. IS under dark conditions.

plus another feature, a plateau at intermediate potentials. This is strong evidence that band unpinning occurs by the charging of a deep surface state as proposed theoretically in section 4. Figures 7–9 compare the capacitance results with and without ZnS coating, and it is observed that the presence of the dielectric film causes a prolongation of the band unpinning to higher potentials, in good agreement with the theoretical predictions of Figure 4. For CBD samples, the plateau region in C_μ is larger, Figure 6b, and is also clearly observed even for non-ZnS coated samples, see Figure 9a, indicating that the layer of QDs grown by CBD also acts as an intermediate layer that amplifies the bandshift. The plateau feature of the capacitance clearly indicates the presence of a surface state that may induce recombination through the monoenergetic level in the bandgap (processes 3 and 4 in Figure 1b). This process should cause a large decrease in the FF of the QDSCs, as previously commented. It should be pointed out that this behavior is not unique to QDSCs. A similar effect has been clearly observed in TiO_2 nanostructured electrodes in aqueous electrolyte without light absorber[53] and also in DSCs with ionic liquid as hole conductor.[62] Therefore the effect cannot be only ascribed to the light absorber and indicates an important role of the electrolyte. Further work is needed to clarify completely the origin of this behavior.
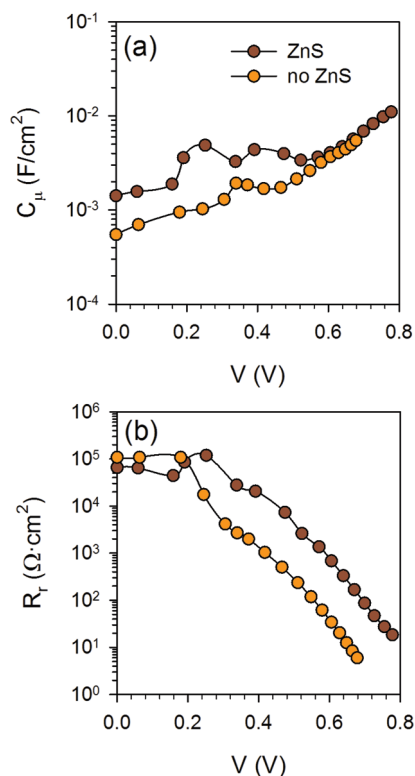

FIGURE 9. (a) Chemical capacitance and (b) recombination resistance as a function of voltage in a QDSC with chemical bath deposited QDs (CBD), with and without ZnS coating, using Au as the counter electrode material. IS under dark conditions.

The recombination resistance of TiO_2 increases significantly with the ZnS treatment, independently of the adsorption method of the QDs, see Figures 7–9. The role of ZnS coating is to reduce the recombination of electrons from TiO_2 into the electrolyte, via the interposition of an intermediate layer. The characteristic pattern of the recombination through a monoenergetic surface state (i.e., a minimum in R_r,[41]) in the recombination resistance can be observed at $V_F \approx 0.2$ V, especially for the LA and CBD samples coated with ZnS, Figures 8b and 9b, respectively.

Figure 6c shows that R_r is always higher for the CBD specimens, due to the higher surface coverage of TiO_2, intrinsic of the CBD preparation, as compared with DA and LA, which exhibit a similar behavior. The same trend occurs in the absence of the ZnS passivation treatment. These results indicate that the CBD method produces a close-packed QD layer that hinders electron recombination in the TiO_2/electrolyte interface due to the presence of an intermediate layer (the QDs themselves), while the TiO_2 surface is amply exposed to the electrolyte for DA and LA QDs.[39]

From this analysis, it should be expected that the CBD samples perform substantially better than colloidal QD samples, since they exhibit both a higher light absorption and a higher

recombination resistance. However, the CBD samples show a moderate 14% increase of photocurrent compared with DA specimens, indicating the presence of an additional recombination channel operating in the CBD samples. This mechanism is not kinetically observed by IS measurements, which means that the recombination channel is faster than 1 μs. The origin of this mechanism could be the internal recombination in the close-packed QD layer produced by CBD (e.g., grain boundary recombination), indicated by process 5 in Figure 1b, which does not operate for the nearly isolated colloidal QDs. Hodes has recently pointed out[4] that thicker semiconductor layers may increase internal recombination in the absorber, and our results agree with this suggestion. A possible strategy to reduce this internal recombination could be to introduce a fast hole scavenger as Ru dye, as proposed in a previous work.[63]

Finally, we discuss the electron lifetime, τ_n, in the QDSCs. This parameter is frequently used to evaluate the solar cell performance. Direct measurements of the electron lifetime extracted from the V_{oc} decay measurements[64,65] are compared with the lifetime calculated from IS, $\tau_n = R_r C_\mu$. Figure 10a shows that the ZnS coating leads to an increase of the electron lifetime in QDSCs, which is expected by the effect of reduced recombination. A good agreement between the lifetime calculated by both techniques is obtained, see Figure 10b, if V_{oc} is shifted around 150 mV for V_{oc} decay data. This fact is an additional indicator of the presence of a surface state that is filled under the illumination conditions of V_{oc} decay, in comparison to the dark conditions of the IS measurements.[66]

7. Conclusion

A systematic analysis of CdSe QDSCs with polysulfide electrolyte using three different QD adsorption strategies, namely, CBD, DA, and LA, shows that the main recombination mechanism is the same as that operating in DSC: the electrons photoinjected into the TiO_2 recombine with the redox couple in the electrolyte. This recombination can be significantly reduced by the interposition of an intermediate layer as a ZnS coating. However, an additional recombination pathway through a monoenergetic surface state, identified by capacitance−voltage results from impedance spectroscopy, causes a strong reduction of the FF and decreases the energy conversion efficiencies of this kind of solar cell. QDSCs prepared by CBD exhibit higher potentialities than colloidal QDSCs due to both their higher recombination resistance and higher light absorption. Nevertheless the relatively low increase in the photocurrent indi-
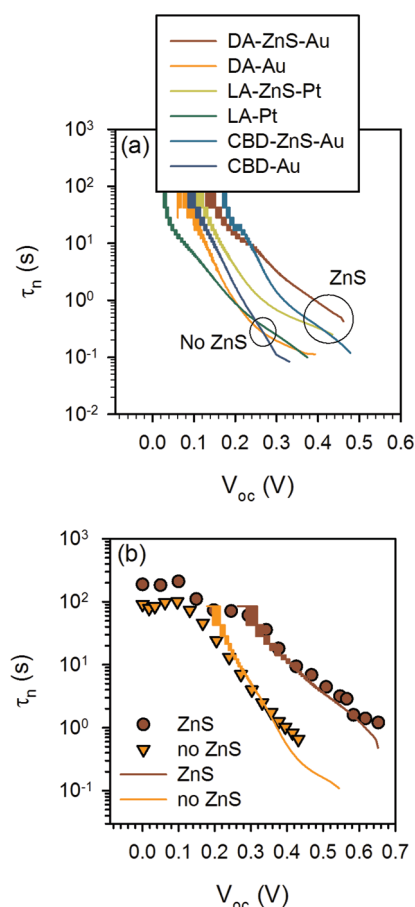

FIGURE 10. (a) Electron lifetime from V_{oc} decay of DA, LA, and CBD samples with and without ZnS coating and (b) comparison between electron lifetime obtained from IS measurements (points) and V_{oc} decay measurements (lines). In the latter, V_{oc} has been shifted a constant value ($\Delta V_{ZnS} = +0.170$ V, $\Delta V_{no\,ZnS} = +0.150$ V), which takes into account the surface state charging under illumination conditions.

cates the presence of additional internal recombination losses in closely packed QDs. Such recombination could be counteracted by faster hole scavengers.

Supporting Information Available. Details of solar cell preparation, stability of CdSe in polysulfide electrolyte, reactivity of the sulfide electrolyte with different counter electrodes, reflectance measurements of QD sensitized electrodes, and the equivalent circuit employed to fit impedance spectroscopy measurements. This material is available free of charge via the Internet at http://pubs.acs.org.

BIOGRAPHICAL INFORMATION

Iván Mora-Seró (1974, M. Sc. Physics 1997, Ph. D. Physics 2004) has been researcher at Universitat Jaume I (Spain) since 2002. He has worked on crystal growth and characterization of nanostructured devices, conducting both experimental and theoretical research. Nowadays he is focused on the study of charge generation and separation in quantum dots and the application in QDSCs.

Sixto Giménez is curently Ramón y Cajal researcher at Department of Physics of the Universitat Jaume I de Castellón. His research is mainly focused on the manufacturing and electrochemical and optoelectronic characterization of QDSC.

Francisco Fabregat Santiago (1970, Bs.C. 1995, Ph.D. in physics 2001) is associate professor at Universitat Jaume I, Spain. He is an expert in electro-optical characterization of devices and particularly known by his studies on the electrical characteristics of nanocolloids, nanorods, nanotubes, dye solar cells, and electrochromic materials using impedance spectroscopy.

Roberto Gómez is associate professor of physical chemistry at the University of Alicante. He has been postdoctoral fellow at Purdue University under the supervision of Prof. M. J. Weaver. He conducts research on the (photo)electrochemistry of semiconductors with a focus on nanostructured electrodes and their application in photocatalysis and third generation solar cells.

Qing Shen received her B.S. (1987) and M.Sc. (1989) in physics from the Nanjing University, China. She received her Ph.D. (1995) in applied chemistry from the Tokyo University, Japan. She is an Assistant Professor in the University of Electro-Communication, Japan. Her research interests include fabrication, characterization and application of metal and semiconductor quantum dots.

Taro Toyoda is a professor of applied physics at the University of Electro-Communications, Japan. He received his B.S. (1970), M.Sc. (1972), and D.Sc. (1975) degrees from the Tokyo Metropolitan University, Japan. His current major research interests include optical properties of semiconductor and metal quantum dots and their applications to photovoltaic devices.

Juan Bisquert (M.Sc. Physics 1985, Ph.D. Physics 1992) is professor of Applied Physics at Universitat Jaume I, Spain. His recent research activity was focused on hybrid and organic photovoltaic devices, in particular dye-sensitized solar cells.

FOOTNOTES

*Corresponding authors. E-mail addresses: sero@fca.uji.es; toyoda@pc.uec.ac.jp; bisquert@fca.uji.es.

REFERENCES

1 Nozik, A. J. Quantum Dot Solar Cells. *Phys. E* **2002**, *14*, 115–200.

2 Klimov, V. I. Mechanisms for Photogeneration and Recombination of Multiexcitons in Semiconductor Nanocrystals: Implications for Lasing and Solar Energy Conversion. *J. Phys. Chem. B* **2006**, *110*, 16827–16845.

3 Kamat, P. V. Quantum Dot Solar Cells. Semiconductor Nanocrystals as Light Harvesters. *J. Phys. Chem. C* **2008**, *112*, 18737–18753.

4 Hodes, G. Comparison of Dye- and Semiconductor-Sensitized Porous Nanocrystalline Liquid Junction Solar Cells. *J. Phys. Chem. C* **2008**, *112*, 17778–17787.

5 Yu, W.; Qu, L. H.; Guo, W. Z.; Peng, X. G. Experimental Determination of the Extinction Coefficient of CdTe, CdSe, and CdS Nanocrystals. *Chem. Mater.* **2003**, *15*, 2854–2860.

6 Wang, P.; Zakeeruddin, S. M.; Moser, J. E.; Humphry-Baker, R.; Comte, P.; Aranyos, V.; Hagfeldt, A.; Nazeeruddin, M. K.; Gratzel, M. Stable New Sensitizer with Improved Light Harvesting for Nanocrystalline Dye-Sensitized Solar Cells. *Adv. Mater.* **2004**, *16*, 1806–1811.

7 Vogel, R.; Pohl, K.; Weller, H. Sensitization of Highly Porous, Polycrystalline TiO2 Electrodes by Quantum Sized CdS. *Chem. Phys. Lett.* **1990**, *174*, 241–246.

8 Vogel, R.; Hoyer, P.; Weller, H. Quantum-Sized PdS, CdS, Ag₂S, Sb₂S₃ and Bi₂S₃ Particles as Sensitizers for Various Nanoporous Wide-Bandgap Semiconductors. *J. Phys. Chem.* **1994**, *98*, 3183–3188.

9 Schaller, R. D.; Sykora, M.; Pietryga, J. M.; Klimov, V. I. Seven Excitons at Cost of One: Redefining the Limits for Conversion Efficiency of Photons into Charge Carriers. *Nano Lett.* **2006**, *6*, 424–429.

10 Trinh, M. T.; Houtepen, A. J.; Schins, J. M.; Hanrath, T.; Piris, J.; Knulst, W.; Goossens, A. P. L. M.; Siebbeles, L. D. A. In Spite of Recent Doubts Carrier Multiplication Does Occur in PbSe Nanocrystals. *Nano Lett.* **2008**, *8*, 1713–1718.

11 O'Regan, B.; Grätzel, M. A Low-Cost High-Efficiency Solar Cell Based on Dye-Sensitized Colloidal TiO2 Films. *Nature* **1991**, *353*, 737–740.

12 Cao, Y.; Bai, Y.; Yu, Q.; Cheng, Y.; Liu, S.; Shui, D.; Gao, F.; Wang, P. Dye-Sensitized Solar Cells with a High Absorptivity Ruthenium Sensitizer Featuring a 2-(Hexylthio)thiophene Conjugated Bipyridine. *J. Phys. Chem. C* **2009**, *113*, 6290–6297.

13 Niitsoo, O.; Sarkar, S. K.; Pejoux, C.; Rühle, S.; Cahen, D.; Hodes, G. Chemical Bath Deposited CdS/CdSe-Sensitized Porous TiO2 Solar Cells. *J. Photochem. Photobiol. A* **2006**, *181*, 306–311.

14 Diguna, L. J.; Shen, Q.; Kobayashi, J.; Toyoda, T. High Efficiency of CdSe Quantum-Dot-Sensitized TiO2 Inverse Opal Solar Cells. *Appl. Phys. Lett.* **2007**, *91*, 023116.

15 Lee, H. J.; Yum, J.-H.; Leventis, H. C.; Zakeeruddin, S. M.; Haque, S. A.; Chen, P.; Seok, S. I.; Grätzel, M.; Nazeeruddin, M. K. CdSe Quantum Dot-Sensitized Solar Cells Exceeding Efficiency 1% at Full-Sun Intensity. *J. Phys. Chem. C* **2008**, *112*, 11600–11608.

16 Diamant, Y.; Chen, S. G.; Melamed, O.; Zaban, A. Core-Shell Nanoporous Electrode for Dye Senxitized Solar Cells: the Effect of the SrTiO₃ Shell on the Electronic Properties of the TiO₂ Core. *J. Phys. Chem. B* **2003**, *107*, 1977–1981.

17 Fabregat-Santiago, F.; García-Cañadas, J.; Palomares, E.; Clifford, J. N.; Haque, S. A.; Durrant, J. R.; Garcia-Belmonte, G.; Bisquert, J. The Origin of Slow Electron Recombination Processes in Dye-Sensitized Solar Cells with Alumina Barrier Coatings. *J. Appl. Phys.* **2004**, *96*, 6903–6907.

18 Law, M.; Greene, L. E.; Radenovic, A.; Kuykendall, T.; Liphardt, J.; Yang, P. ZnO—Al₂O₃ and ZnO—TiO₂ Core—Shell Nanowire Dye-Sensitized Solar Cells. *J. Phys. Chem. B* **2006**, *110*, 22652–22663.

19 Shen, Q.; Kobayashi, J.; Diguna, L. J.; Toyoda, T. Effect of ZnS Coating on the Photovoltaic Properties of CdSe Quantum Dot-Sensitized Solar Cells. *J. Appl. Phys.* **2008**, *103*, 084304.

20 Giménez, S.; Mora-Seró, I.; Macor, L.; Guijarro, N.; Lana-Villarreal, T.; Gómez, R.; Diguna, L. J.; Shen, Q.; Toyoda, T.; Bisquert, J. Improving the Performance of Colloidal Quantum-Dot-Sensitized Solar Cells. *Nanotechnology* **2009**, *20*, 295204.

21 Kelly, J. J.; Memming, R. The Influence of Surface Recombination and Trapping on the Cathodic Photocurrent at p-type III-V Electrodes. *J. Electrochem. Soc.* **1982**, *192*, 730–738.

22 Nozik, A. J. Exciton Multiplication and Relaxation Dynamics in Quantum Dots: Applications to Ultrahigh-Efficiency Solar Photon Conversion. *Inorg. Chem.* **2005**, *44*, 6893–6899.

23 Serpone, N.; Borgarello, E.; Grätzel, M. Visible Light Induced Generation of Hydrogen from Hydrogen Sulfide in Mixed Semiconductor Dispersions; Improved Efficiency through Inter-Particle Electron Transfer. *J. Chem. Soc., Chem. Commun.* **1995**, *6*, 342–344.

24 Liu, D.; Kamat, P. V. Photoelectrochemical Behavior of Thin CdSe and Coupled TiO₂/CdSe Semiconductor Films. *J. Phys. Chem.* **1993**, *97*, 10769–10773.

25 Zaban, A.; Micic, O. I.; Gregg, B. A.; Nozik, A. J. Photosensitization of Nanoporous TiO₂ Electrodes with InP Quantum Dots. *Langmuir* **1998**, *14*, 3153–3156.

26 Gorer, S.; Hodes, G. Quantum-Size Effects in the Study of Chemical Solution Deposition Mechanims of Semiconductor Films. *J. Phys. Chem.* **1994**, *98*, 5338–5346.

27 Nicolau, Y. F. Solution Deposition of Thin Solid Compound Films by a Successive Ionic-Layer Adsorption and Reaction Process. *Appl. Surf. Sci.* **1985**, *22—3*, 1061–1074.

28 Nicolau, Y. F.; Dupuy, M.; Brunel, M. ZnS, CdS, and Zn1-XCdXS Thin-Film Deposited by the Successive Ionic Layer Adsorption and Reaction Process. *J. Electrochem. Soc.* **1990**, *137*, 2915–2924.

29 Robel, I.; Subramanian, V.; Kuno, M.; Kamat, P. V. Quantum Dot Solar Cells. Harvesting Light Energy with CdSe Nanocrystals Molecularly Linked to Mesoscopic TiO$_2$ Films. *J. Am. Chem. Soc.* **2006**, *128*, 2385–2393.

30 López-Luque, T.; Wolcott, A.; Xu, L. P.; Chen, S.; Wen, Z.; Li, J.; De la Rosa, E.; Zhang, J. Z. Nitrogen-Doped and CdSe Quantum-Dot-Sensitized Nanocrystalline TiO$_2$ Films for Solar Energy Conversion Applications. *J. Phys. Chem. C* **2008**, *112*, 1282–1292.

31 Leschkies, S. K.; Divakar, R.; Basu, J.; Enache-Pommer, E.; Boercker, J. E.; Carter, C. B.; Kortshagen, U. R.; Norris, D. J.; Aydil, E. S. Photosensitization of ZnO Nanowires with CdSe Quantum Dots for Photovoltaic Devices. *Nano Lett.* **2007**, *7*, 1793–1798.

32 Mora-Seró, I.; Giménez, S.; Moehl, T.; Fabregat-Santiago, F.; Lana-Villareal, T.; Gómez, R.; Bisquert, J. Factors Determining the Photovoltaic Performance of a CdSe Quantum Dot Sensitized Solar Cell: The Role of the Linker Molecule and of the Counter Electrode. *Nanotechnology* **2008**, *19*, 424007.

33 Kongkanand, A.; Tvrdy, K.; Takechi, K.; Kuno, M.; Kamat, P. V. Quantum Dot Solar Cells. Tuning Photoresponse through Size and Shape Control of CdSe–TiO$_2$ Architecture. *J. Am. Chem. Soc.* **2008**, *130*, 4007–4015.

34 Guijarro, N.; Lana-Villarreal, T.; Mora-Seró, I.; Bisquert, J.; Gómez, R. CdSe Quantum Dot Sensitized TiO$_2$ Electrodes: Effect of QD Coverage and Mode of Attachment. *J. Phys. Chem. C* **2009**, *113*, 4208–4214.

35 Lin, S.-C.; Lee, Y.-L.; Chang, C.-H.; Shen, Y.-J.; Yang, Y.-M. Quantum-Dot-Sensitized Solar Cells: Assembly of CdS-Quantum-Dots Coupling Techniques of Self-Assembled Monolayer and Chemical Bath Deposition. *Appl. Phys. Lett.* **2007**, *90*, 143517.

36 Lee, Y.-L.; Huang, B.-M.; Chien, H.-T. Highly Efficient CdSe-Sensitized TiO$_2$ Photoelectrode for Quantum-Dot-Sensitized Solar Cell Applications. *Chem. Mater.* **2008**, *20*, 6903–6905.

37 Shen, Y.; Bao, J.; Dai, N.; Wu, J.; Gu, F.; Tao, J. C.; Zhang, J. C. Speedy Photoelectric Exchange of CdSe Quantum Dots/Mesoporous Titania Composite System. *Appl. Surf. Sci.* **2009**, *255*, 3908–3911.

38 Yu, P.; Zhu, K.; Norman, A. G.; Ferrere, S.; Frank, A. J.; Nozik, A. J. Nanocrystalline TiO$_2$ Solar Cells Sensitized with InAs Quantum Dots. *J. Phys. Chem. B* **2006**, *110*, 25451–25454.

39 Guijarro, N.; Lana-Villarreal, T.; Mora-Seró, I.; Bisquert, J.; Gómez, R. CdSe Quantum Dot Sensitized TiO$_2$ Electrodes: Effect of QD Coverage and Mode of Attachment. *J. Phys. Chem. C* **2009**, *113*, 4208–4214.

40 Shalom, M.; Dor, S.; Rühle, S.; Grinis, L.; Zaban, A. Core/CdS Quantum Dot/Shell Mesoporous Solar Cells with Improved Stability and Efficiency Using an Amorphous TiO$_2$ Coating. *J. Phys. Chem. C* **2009**, *113*, 3895–3898.

41 Mora-Sero, I.; Bisquert, J. Fermi Level of Surface States in TiO$_2$ Nanoparticles. *Nano Lett.* **2003**, *3*, 945–949.

42 Lee, Y.-L.; Chang, C.-H. Efficient Polysulfide Electrolyte for CdS Quantum Dot-Sensitized Solar Cells. *J. Power Sources* **2008**, *185*, 584–588.

43 Shen, Q.; Arae, D.; Toyoda, T. Photosensitization of Nanostructured TiO2 with CdSe Quantum Dots: Effects of Microstructure and Electron Transport in TiO2 Substrates. *J. Photochem. Photobiol. A* **2004**, *164*, 75–80.

44 Shen, Q.; Toyoda, T. Characterization of Nanostructured TiO2 Electrodes Sensitized with CdSe Quantum Dots Using Photoacoustic and Photoelectrochemical Current Methods. *Jpn. J. Appl. Phys.* **2004**, *43*, 2946–2951.

45 Shen, Q.; Katayama, K.; Yamaguchi, M.; Sawada, T.; Toyoda, T. Study of Ultrafast Carrier Dynamics of Nanostructured TiO2 Films with and without CdSe Quantum Dot Deposition Using Lens-Free Heterodyne Detection Transient Grating Technique. *Thin Solid Films* **2005**, *486*, 15–19.

46 Shen, Q.; Katayama, K.; Sawada, T.; Yamaguchi, M.; Toyoda, T. Optical Absorption, Photoelectrochemical, And Ultrafast Carrier Dynamic Investigations of TiO2 Electrodes Composed of Nanotubes and Nanowires Sensitized with CdSe Quantum Dots. *Jpn. J. Appl. Phys.* **2006**, *45*, 5569–5575.

47 Shen, Q.; Sato, T.; Hashimoto, M.; Chen, C. C.; Toyoda, T. Photoacoustic and Photo-Electrochemical Characterization of Cdse-Sensitized TiO2 Electrodes Composed of Nanotubes and Nanowires. *Thin Solid Films* **2006**, *499*, 299–305.

48 Diguna, L. J.; Shen, Q.; Sato, A.; Katayama, K.; Sawada, T.; Toyoda, T. Optical Absorption and Ultrafast Carrier Dynamics Characterization of CdSe Quantum Dots Deposited on Different Morphologies of Nanostructured TiO2 Films. *Mater. Sci. Eng., C* **2007**, *27*, 1514–1520.

49 Shen, Q.; Yanai, M.; Katayama, K.; Sawada, T.; Toyoda, T. Optical Absorption, Photosensitization, And Ultrafast Carrier Dynamic Investigations of CdSe Quantum Dots Grafted onto Nanostructured SnO2 and Fluorine-Doped Tin Oxide (FTO) Glass. *Chem. Phys. Lett.* **2007**, *442*, 89–96.

50 Hines, M. A.; Guyot-Sionnest, P. Synthesis and Characterization of Strongly Luminescing ZnS-Capped CdSe Nanocrystals. *J. Phys. Chem.* **1996**, *100*, 468–471.

51 Bisquert, J. Chemical Capacitance of Nanostructured Semiconductors: Its Origin and Significance for Heterogeneous Solar Cells. *Phys. Chem. Chem. Phys.* **2003**, *5*, 5360–5364.

52 Cowley, A. M. Depletion Capacitance and Diffusion Potential of Gallium Phosphide Schottky-Barries Diode. *J. Appl. Phys.* **1966**, *37*, 3024–3032.

53 Bisquert, J.; Fabregat-Santiago, F.; Mora-Seró, I.; Garcia-Belmonte, G.; Barea, E. M.; Palomares, E. A Review of Recent Results on Electrochemical Determination of the Density of Electronic States of Nanostructured Metal-Oxide Semiconductors and Organic Hole Conductors. *Inorg. Chim. Acta* **2008**, *361*, 684–698.

54 Bisquert, J.; Zaban, A. The Trap-Limited Diffusivity of Electrons in Nanoporous Semiconductor Networks Permeated with a Conductive Phase. *Appl. Phys. A* **2003**, *77*, 507–514.

55 Boschloo, G.; Fitzmaurice, D. Spectroelectrochemical Investigation of Surface States in Nanostructured TiO$_2$ Electrodes. *J. Phys. Chem. B* **1999**, *103*, 2228–2231.

56 Berger, T.; Lana-Villarreal, T.; Monllor-Satoca, D.; Gomez, R. An Electrochemical Study on the Nature of Trap States in Nanocrystalline rutile Thin Films. *J. Phys. Chem. C* **2007**, *111*, 9936–9942.

57 Bisquert, J.; Zaban, A.; Salvador, P. Analysis of the Mechanism of Electron Recombination in Nanoporous TiO2 Dye-Sensitized Solar Cells. Nonequilibrium Steady State Statistics and Transfer Rate of Electrons in Surface States. *J. Phys. Chem. B* **2002**, *106*, 8774–8782.

58 Wang, Q.; Ito, S.; Grätzel, M.; Fabregat-Santiago, F.; Mora-Seró, I.; Bisquert, J.; Bessho, T.; Imai, H. Characteristics of High Efficiency Dye-sensitized Solar Cells. *J. Phys. Chem. B* **2006**, *110*, 19406–19411.

59 Fabregat-Santiago, F.; Bisquert, J.; Palomares, E.; Otero, L.; Kuang, D.; Zakeeruddin, S. M.; Grätzel, M. Correlation between Photovoltaic Performance and Impedance Spectroscopy of Dye-Sensitized Solar Cells Based on Ionic Liquids. *J. Phys. Chem. C* **2007**, *111*, 6550–6560.

60 Mora-Seró, I.; Bisquert, J.; Fabregat-Santiago, F.; Garcia-Belmonte, G.; Zoppi, G.; Durose, K.; Proskuryakov, Y.; Oja, I.; Belaidi, A.; Dittrich, T.; Tena-Zaera, R.; Katty, A.; Lévy-Clément, C.; Barrioz, V.; Irvine, S. J. C. Implications of the Negative Capacitance Observed at Forward Bias in Nanocomposite and Polycrystalline Solar Cells. *Nano Lett.* **2006**, *6*, 640–650.

61 Bisquert, J.; Garcia-Belmonte, G.; Montero, J. M.; Bolink, H. Charge Injection in Organic Light Emitting Diodes Governed by Interfacial States. *Proc. SPIE Int. Soc. Opt. Eng.* **2006**, *6192*, 619210.

62 Randriamahazaka, H.; Fabregat-Santiago, F.; Zaban, A.; García-Cañadas, J.; Garcia-Belmonte, G.; Bisquert, J. Chemical Capacitance of Nanoporous- Nanocrystalline TiO2 in a Room Temperature Ionic Liquid. *Phys. Chem. Chem. Phys.* **2006**, *8*, 1827–1833.

63 Mora-Seró, I.; Dittrich, T.; Susha, A. S.; Rogach, A. L.; Bisquert, J. Large Improvement of Electron Extraction from CdSe Quantum Dots into a TiO2 Thin Layer by N3 Dye Coabsorption. *Thin Solid Films* **2008**, *516*, 6994–6998.

64 Zaban, A.; Greenshtein, M.; Bisquert, J. Determination of the Electron Lifetime in Nanocrystalline Dye Solar Cells by Open-Circuit Voltage Decay Measurements. *ChemPhysChem* **2003**, *4*, 859–864.

65 Bisquert, J.; Zaban, A.; Greenshtein, M.; Mora-Seró, I. Determination of Rate Constants for Charge Transfer and the Distribution of Semiconductor and Electrolyte Electronic Energy Levels in Dye-Sensitized Solar Cells by Open-Circuit Photovoltage Decay Method. *J. Am. Chem. Soc.* **2004**, *126*, 13550–13559.

66 Bisquert, J. Analysis of the Kinetics of Ion Intercalation. Ion Trapping Approach to Solid-State Relaxation Processes. *Electrochim. Acta* **2002**, *47*, 2435–2449.